

# PALEOSEISMIC FAULTING AND LANDSLIDES TRIGGERED BY EARTHQUAKES IN ECUADOR FROM AIRBORNE AND SPACEBORNE IMAGES

Alessandro Tibaldi

Dipartimento di Scienze della Terra, Università degli Studi di Milano, 20133 - Italia

## ABSTRACT

Enhanced Landsat, radar images and aerial stereophotos were coregistered with topographical data of Ecuadorian Andes at 1:50,000 scale to identify morphological and geological indicators of paleoseismic faulting. From the same data a map of landslides triggered by the March 5, 1987 earthquake was prepared and digitized. A comparison was made between the location and density of active faults, epicentres, landslides, surficial deposits and mountain slope inclination and orientation. The main results which were mostly based on remotely-sensed data are a map depicting the scenario of recent and active tectonics and gravitational instability and also the discovering of a preferred distribution of landslides with respect to the fault and mountain slope dip. This study shows that coregistration of remotely-sensed and geodata is a good procedure to assist seismic and landslide hazard.

KEY WORDS: Landsat, Radar, Stereophotos, Mapping, Paleoseismic Faults, Landslides.

## 1. INTRODUCTION

During the last twenty years as many lineament maps as at least are the faults in the Alps were prepared. Between "lineament" and "fault" there is an important difference and probably many tectonic maps derived from remotely-sensed data lack of field checks. One of the most important reasons for this lacking was the difficulty for precise location of lineaments on topographical maps. During the last years, improvements in sensor resolution and computer techniques allowed the digital superimposing of remotely-sensed data with topographic data at a scale up to 1:50,000 or better. In this way field checks can and must be done anyway and faults can be compared with seismological data. This last statement is particularly important because it may be possible on high resolution images to recognize geomorphological indicators of recent and active fault motions.

In this paper the potential of remotely-sensed data for the recognition and location of paleoseismic faults is explored throughout the Ecuadorian Andes (EA). Airborne and spaceborne images are also used to quantify the distribution of landslides triggered by two events (Magnitude of surface wave 6.9 and 6.1) that occurred on March 5, 1987 in the northern part of the EA. Coregistration of these data sets with topographical, surficial deposits and geophysical maps permits a semi-automatic comparison with slope inclination and orientation, rheological characteristics of rocks, epicentre distribution, and isoseism patterns.

## 2. SPACEBORNE AND AIRBORNE DATA AND DIGITAL TECHNIQUES

The satellite data set comprises eleven Landsat MSS images at 1:500,000 scale and one CCT. The used band was the near infrared (0.8-1.1 micron). From the CCT four subscenes were computer enlarged at 1 : 100,000 scale and contrast stretched. The airborne radar data comprise 8 images at 1 : 80,000 scale. They were obtained with a Synthetic Aperture Radar of CLIRSEN (Centro de Levantamientos Integrados de Recursos Naturales por Sensores Remotos, Quito) with a

Goodyear system. The used band was X (3.12 cm) and sensor resolution 10 meters. Incidence azimuth was westward with two different angles (Far and Near Range). The radar images were especially useful in those areas where cloud covering and jungle density were too high.

Black and white aerial photographs have also been used. They consist in 75 stereoscopic photos at 1 : 80,000 scale, 352 at 1 : 40,000 scale and 12 at 1 : 20,000 scale. They were taken during flights before the 1987 earthquake and afterwards.

The 1 : 50,000 topographical maps were partly published by the "Instituto Geografico Militar" of Ecuador, while the area affected by the landslides of the 1987 earthquake was covered with 1 : 50,000 topographical maps appositely prepared from the aerial stereophotos. All the topographic maps were digitized.

Each image and stereophoto was coregistered with the digitized topographical data. Digital coregistration minimized problems deriving from use of different scale products and allowed some semi-automatic statistical treatment of the data. Epicentres of 122 earthquakes extracted from the NOAA, CERESIS (1986) and OAQ (1981) catalogues were also coregistered, as well as isoseism patterns (Barberi et al., 1988), and surficial deposit distribution (DGGM, 1978; INECEL, 1989; Tibaldi, 1990)

Positive prints of spaceborne and airborne data were fixed on a digitizer after recognition on the computer monitor, showing the topographic data, and on the prints of at least three known benchmarks. A digital pen was used to test the coincidence of the reference points. In this case tracing the paleoseismic faults and landslides was directly performed on the digitizer. The enhanced CCT subscenes were visualized on the computer monitor and, after coregistration with the topographic data through reference points, directly interpreted. According to the resolution of the computer system, the used images, and the general scale of working, a resolution error in the location of interpreted data was estimated

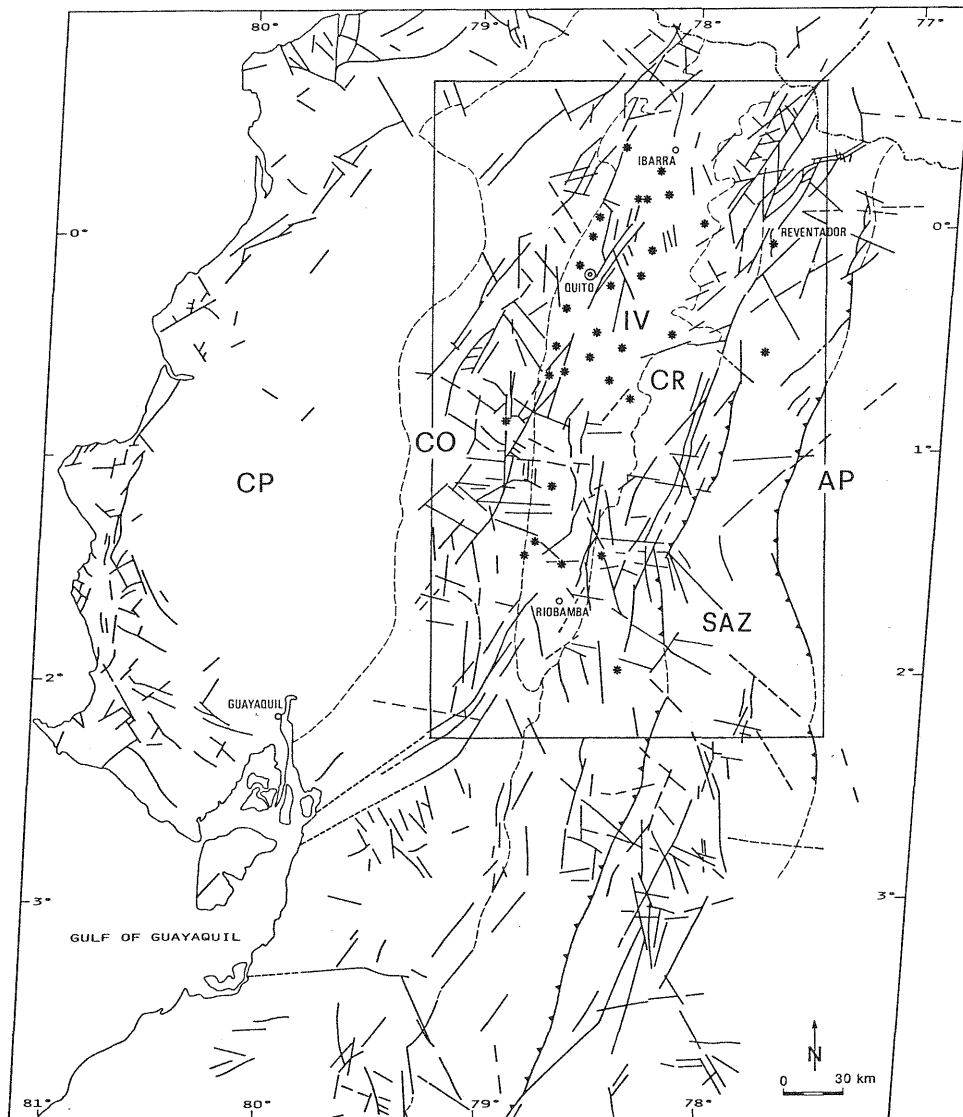


Figure 1. Tectonic map of Ecuador of medium and long lineaments ( $\geq 10$  km) from an interpretation of 1 : 500,000 and 1 : 250,000 scale Landsat MSS images. Asterisks represent Quaternary volcanoes. Boxed area = Figure 2. CP Coastal Plain, CO Cordillera Occidental, IV Interandean Valley, CR Cordillera Real, SAZ Sub-Andean Zone, AP Amazon Platform.

< 30-50 meters.

### 3. EXTRACTION OF PALEOSEISMIC DATA

The complete scenario of the main remotely-sensed faults, integrated with the field checks, is presented in the tectonic map of Fig. 1. In the Coastal Plain of Ecuador (CP in Fig. 1) various sets of short and medium faults (length < 40 km) are present. Some field checks showed that the main part is characterized by reverse motions. Towards the east faults are buried by Quaternary continental deposits. The Cordillera Occidental (CO) is disrupted mainly by NNE-SSW and WNW-ESE faults. In the Interandean Valley (IV) N-S and NNE-SSW faults with normal-oblique motions are widespread (length mainly 10-40 km in CO e IV). The outstanding feature of the Cordillera Real (CR) is a marked and straight family of faults with an overall trend of N 30° (length mainly > 40 km). Field checks show that these faults are vertical or have a dominant dip towards WNW.

Only a little part among these faults show recent tectonic activity. The typical indicator of paleoseismic fault motions is the dislocation of geomorphic features. For example, this comprises up-facing slope brakes, marked not eroded scarps resembling "knife-cuts", dislocation of river streams, gullies, ridges and crests. The amount of these dislocations commonly is in order of Dm-m, while some main faults may accommodate large rates of tectonic motions, in order of tens or hundreds of meters during Holocene times. Theoretically, this means that with the 80 m resolution of the Landsat MSS, only main paleoseismic faults can be detected. In Ecuador it has been noticed that only in rare cases morphological dislocations are detectable even if the total amount is less than 80 m. This situation was recognized when fault escarpments and landslides triggered along the fault trace are creating a linear abrupt changing between fresh outcropping rocks (high reflectance) and dense jungle (high absorption).

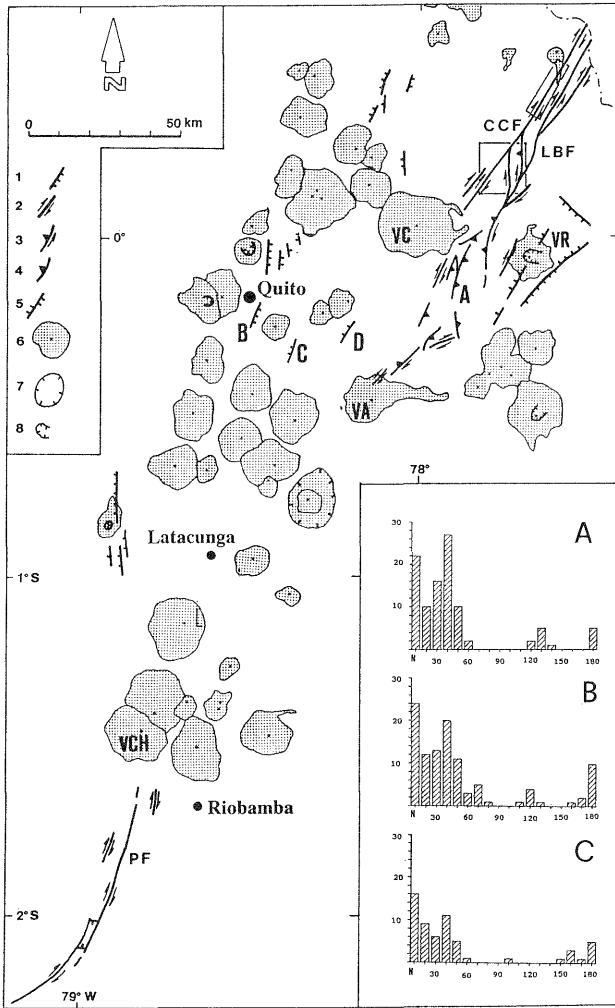


Figure 2. Remotely-sensed (Landsat, SLAR and aerial stereophotos) main recent and active faults of the Ecuadorian Andes checked in the field. Histograms show total number of remote-sensed faults (Y axis) versus azimuth (X axis) for northern (A), central (B) and southern (C) part of the area. Faults: 1 normal, 2 strike-slip, 3 oblique-reverse, 4 reverse, 5 pivotal, CCF Cayambe-Chingual, LBF La Bonita, PF Paillatanga, A, B, C and D referred in the text. Volcanoes: 6 Quaternary, 7 caldera, 8 collapse rim, VC Cayambe, VR Reventador, VA Antisana, VCH Chimborazo. Boxes: square = figure 4; rectangle = figure 5.

Seven main faults with paleoseismic characteristics in the EA were discovered on satellite images. The Cayambe-Chingual Fault (CCF in Fig. 2), named after Tibaldi (1990), can be followed on the image for 76 km. Along the majority of this fault trace, dislocation of river streams and gorges can be measured (Fig. 3), giving a mean value of 360 m. The high altitude of the studied area, ranging between 2,000 and more than 4,000 m, is consistent with the assumption that landforms were inherited from the last main glacial pulses (11,000 ± 1,000 yr BP for the areas > 3,800 m, 27,500 ± 7,500 yr BP for the areas > 3,000 m, Clapperton and Vera, 1986). Considering that the majority of the CCF outcrops between 2,700 and 3,500 m, its horizontal rate of tectonic

motions may be estimated to be 13 ± 2.7 mm/y. The type of faulting was strike-slip right-lateral, according to the sense of river dislocation. The coregistration of this fault trace on the topographical map shows that the analysis on the satellite data is correct both for sense and amount of dislocation (fig. 3 and 4). The same features were discovered along the La Bonita fault (LBF in Fig. 2). Here the Holocene fault motion rate is quite uncertain because only two dislocation amounts have been measured (Fig. 3).

Southward, only a segment of an active N-S fault was recognized on satellite images (site A in Fig. 2). An escarpment facing westward dislocates glacial morphologies of the last pulse revealing relative upward motions of the east block. Topographic data indicates along this segment a total amount of vertical dislocation of about 30 m (a rate of 2.7 ± 0.2 mm/y).

More southward, the eastern Andes are occupied by large volcanoes until the latitude of 2°S. South of this area, a fault with the same characteristics of the CCF can be traced for about 100 km. This fault, named Paillatanga Fault after Winter and Lavenu (1989) (PF in Fig. 2), shows an average dislocation of crests and river streams of 45 m (a rate of 4 ± 0.3 mm/y) (Fig. 3). Motions were strike-slip right-lateral and fault strike goes from NNE to NE.

In the IV some N-S escarpments bordering depressed areas infilled by alluvial or pyroclastic rocks have been recognized on satellite images. The total amount of vertical dislocation is of about 200 m for the fault labelled B in Fig. 2, 150 m for C and 80 m for D.

Using radar images and aerial stereophotos other 36 active faults were discovered (Fig. 2). For example, the segment A was recognized as belonging to a longer NNE fault with a vertical dislocation diminishing northward and

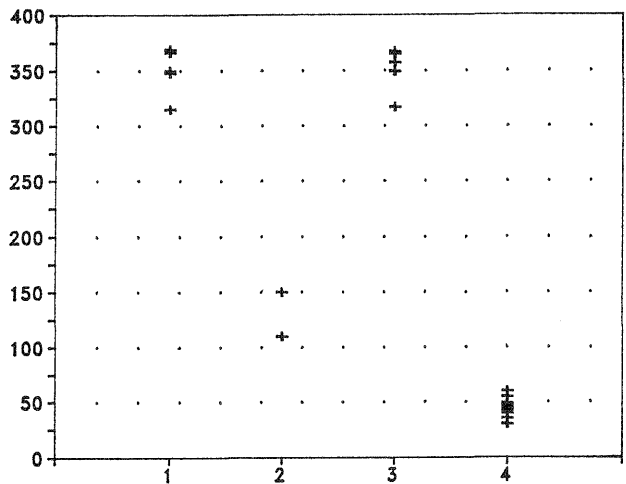


Figure 3. Examples of dislocations in meters (Y axis) measured at different points along some main active faults of the Ecuadorian Andes (X axis) on remote sensed images (1 = Cayambe-Chingual Fault, 2 = La Bonita Fault, 4 = Paillatanga Fault) and with topographical data (3 = Cayambe-Chingual Fault).

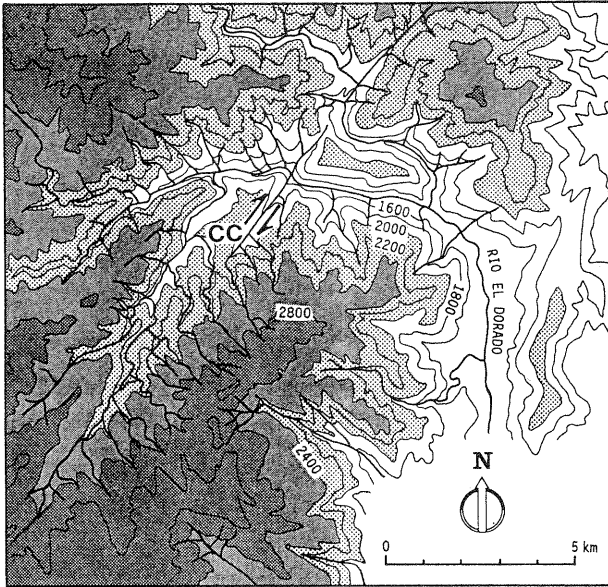


Figure 4. Turning of the tributaries for drag effects along the Cayambe-Chingual Fault. Distortion of the hydrographic pattern is consistent with the right-lateral strike-slip motions detected on the slickenside fault planes. Location on Figure 2.

southward. Measurements of dislocation amount was extended to all these faults and a checking was made on the faults recognized on the satellite images. As an example, the CCF produces an off-set of 1 km in late Pleistocene lava flow (Fig. 5). The resulting dislocation rate of 6 mm/yr (considering 0.16 Ma a representative age for the lava flow) could be consistent with that one measured by the satellite images. Absolute datings could help to constrain these data. Field checks showed that the minimum amount of dislocation usually recognized was of the order of 3-4 m, and confirmed that the escarpments were due to strike-slip or reverse faulting in the eastern Andes and to normal motions in the IV.

These data are consistent with the widespread seismic activity comprising 7 large earthquakes (estimated intensity of Mercalli scale > IX) occurred in the study area (Fig. 6, Observatorio Astronomico de Quito, 1959).

#### 4. LANDSLIDE MAPPING

Several small landslides are located along the major active faults (example in Fig. 5). This distribution is consistent with the presence of active tectonic motions along these faults. Several other landslides of various size have been triggered by the 1987 earthquake and are widespread in the north-eastern EA. The landslides are easily distinguishable on the various images and photos for the high difference of reflectance between the outcropping rocks and the surrounding jungle. The 1987 landslides were mapped on aerial stereophotos to obtain the maximum amount of data. The limit of each landslide was digitized and the affected area was calculated, using a grid cell of 1 sq. km (Fig. 7). The isolines, expressed as percentage of landslided area respect to the cell area, define a NNE elongated zone which is coincident with the

active faults (Fig. 2), with the shape of the areas affected by microseismicity recorded during the periods January-April 1981 (1 in Fig. 6) and December 1986-March 1987 (2 and 3 in Fig. 6) (Barberi et al., 1988)

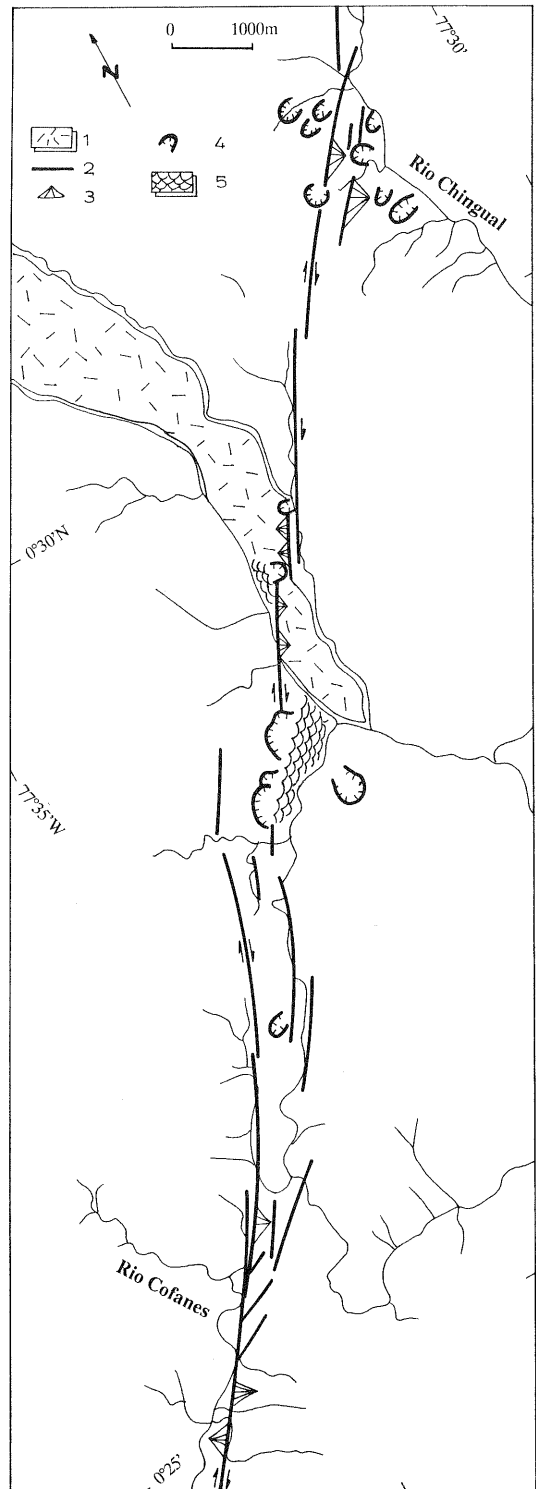


Figure 5. Geomorphic and geological indicators of recent motions along the Cayambe-Chingual Fault. 1. Recent lava flow; 2. fault trace; 3. triangular facets; 4. landslide scarp; 5. large landslide scree-tongue. Location on Figure 2.

and with the isoseismes (Fig. 8). Landslides reach a density of 100% in the central area. The reliability of the isoline shape is supported by the following data: i) variations of slope dip above an inclination of 20-30° did not influence the landslide distribution, ii) the average slope steepness of the landslided area is almost equal to the conterminous zones except eastwards where it gradually passes to the Amazon Platform, iii) isolines crossing the geological limits show a minimum influence of changes in rheological characteristics of rocks.

Comparison of landslide distribution with topography, in the sense of slope orientation and inclination, shows that landsliding was denser along the slopes facing ESE. This discovery is particularly interesting because the geometry

of slope failures could be linked to the dominant WNW dip of active fault planes (for geometry of active faults see also the focal mechanism solutions of Fig. 6 and Pasquarè et al., 1990). If this relationship will be confirmed in other areas, it could represent a stimulating topic for further seismic studies.

## 5. CONCLUSIONS

The integrated use of aerial stereophotos and radar and satellite images enabled to recognize recent fault motions and several landslides triggered by earthquakes in the Ecuadorian Andes. Coregistration and comparison of these data with topographical and geological maps allowed to reach the following results:

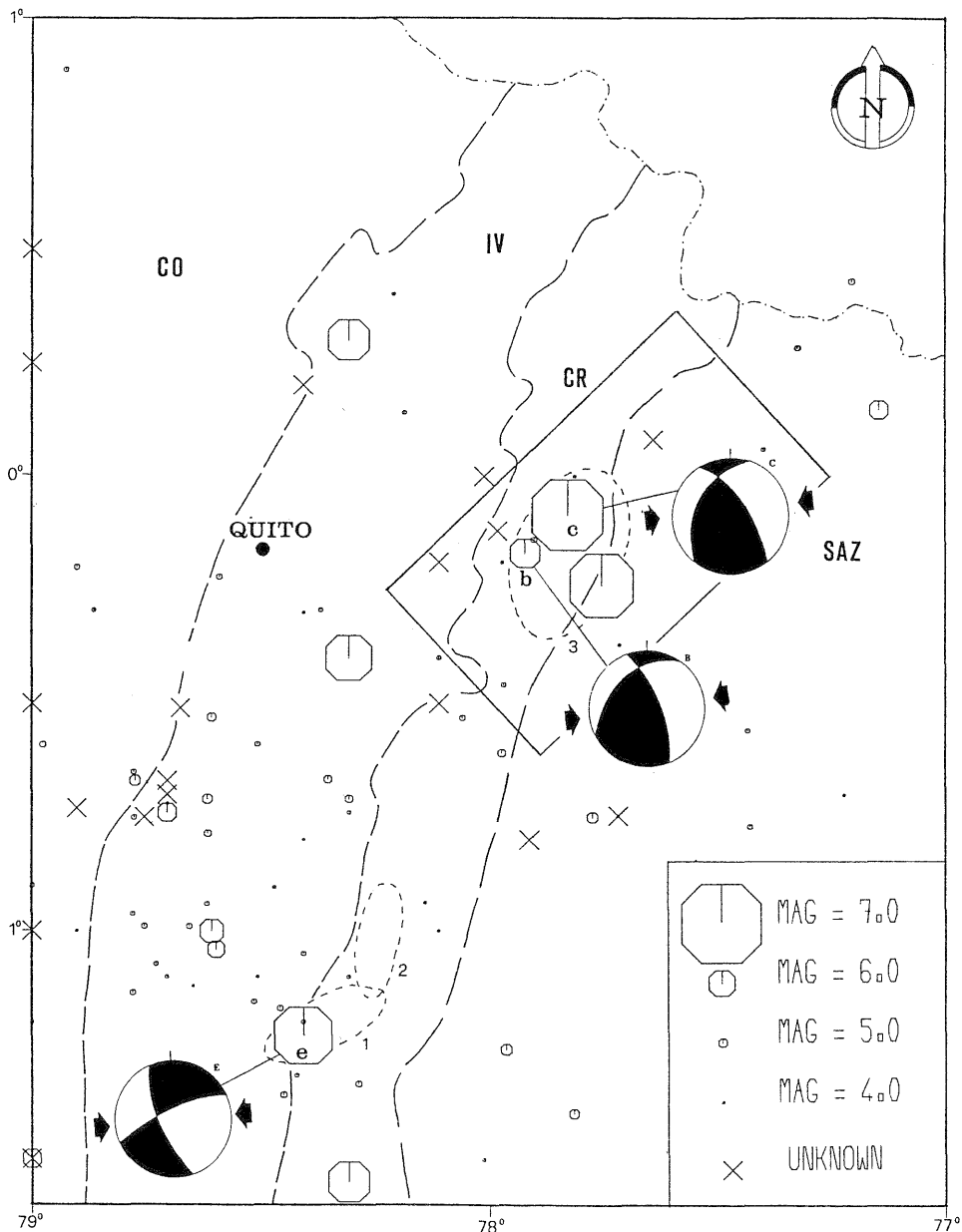


Figure 6. Epicentre distribution map of period 1903-1987. Numbers 1, 2 e 3 refer to microseismicity analyses discussed in the text. Letters refer to focal mechanisms: b and c after Barberi et al. (1988), e after Woodward & Clyde (1981); Black arrows show the horizontal direction of the P axis; Schmidt projection, lower hemisphere. CO Cordillera Occidental, IV Interandean Valley, CR Cordillera Real, SAZ Sub-Andean Zone. Box = figure 7.

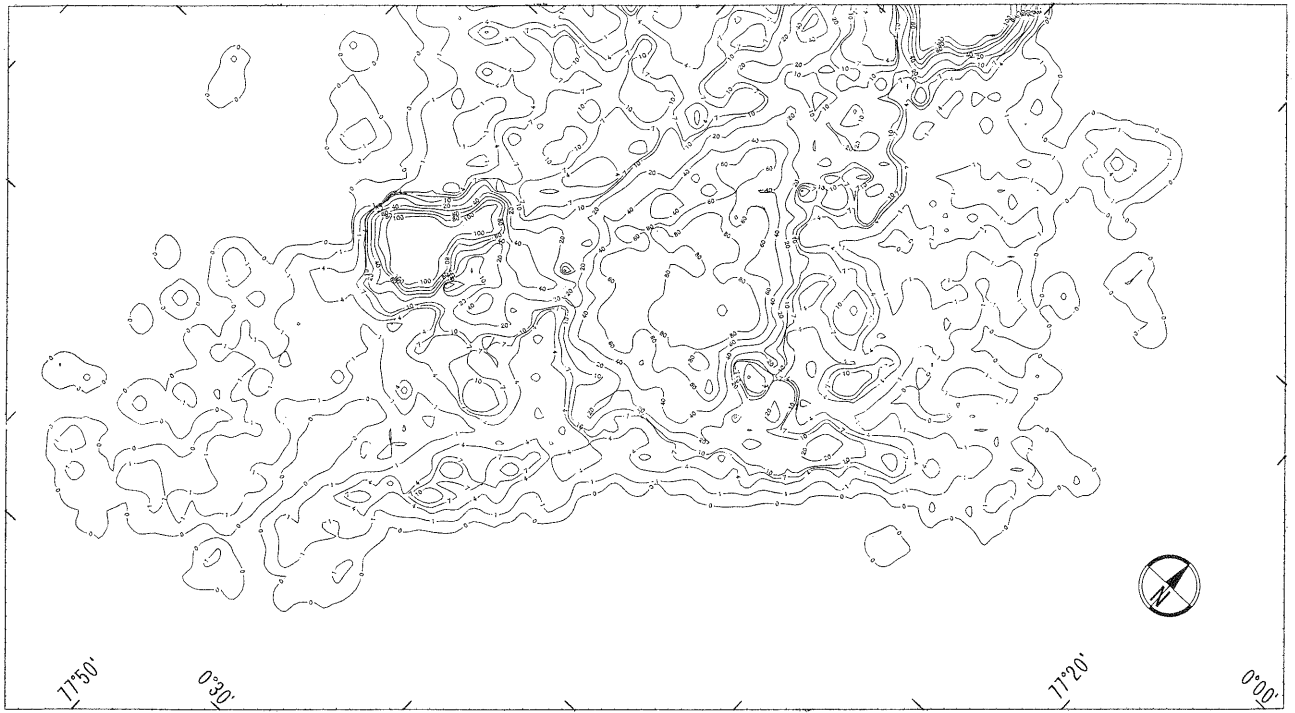


Figure 7. Isolines of the percentage of landslided area measured with grid cells of 1 sq. km (0, 1, 4, 7, 10, 20, 40, 60, 80, 100%). Location on figure 6.

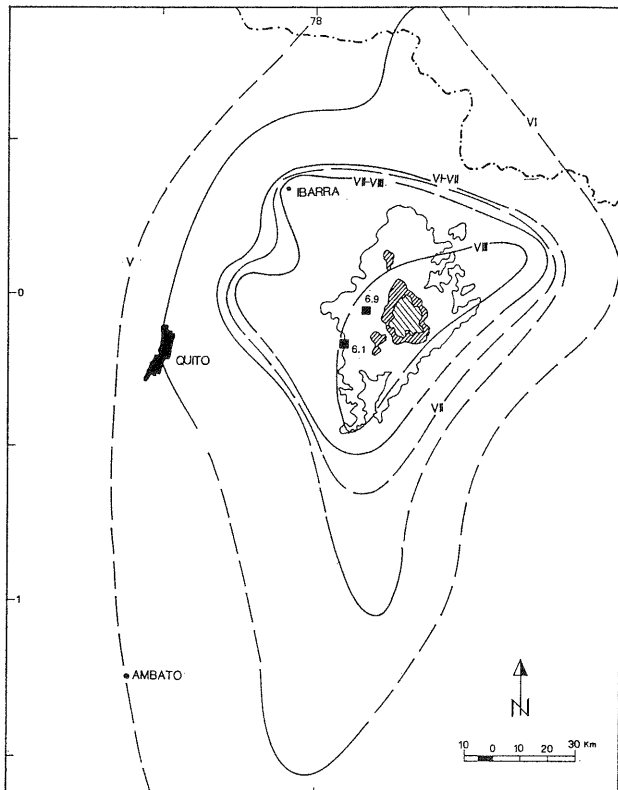


Figure 8. Isoseism map of the 5th March, 1987 earthquake (after Barberi et al., 1988). The degree of intensity is indicated for each line. Black boxes represent the two main shock epicentres with magnitude (M<sub>sw</sub>). The smaller sinuous lines are three isolines encircling areas of landsliding different density (1-49%, 50-99% and 100%).

- 1) the main active faults were identified and the average dislocation rate and sense of motions quantified where possible;
- 2) landslides triggered by earthquakes were mapped and quantified;
- 3) isoline shape of the area affected by landslides coincides with the orientation of the active faults, of isoseismes and of microseismicity, while its maximum density is very close to the related earthquake epicentres;
- 4) the mountain slopes facing ESE show the highest concentration of landslides; comparison of this distribution with the dominant WNW active fault dip could be a good topic for further seismic analyses.

This study shows, in my opinion, that coregistration of remotely-sensed, topographical and geological data is a good procedure to assist seismic and landslide hazard.

#### ACKNOWLEDGMENTS

I am indebted with L. Ferrari and G. Pasquarè for field assistance and with A. Cavallin for cooperation in some of the computer elaborations. The author benefited of a Ph.D. grant from Ministero Italiano della Pubblica Istruzione and from Istituto Nazionale di Geofisica - Gruppo Nazionale per la Vulcanologia.

#### REFERENCES

- Barberi, F., Belloni, L., Ferrari, L., Pasquarè, G., Previtali, F., Tibaldi, A. and Zonno, G., 1988. Riesgo Sismico. Technical Report Coca-Codo Sinclair Project, Quito, Ecuador.
- CERESIS, 1986. Catalogo de terremotos para America del Sur. Datos de hipocentros y intensidades.

Clapperton, C.M. and Vera, R., 1986. The Quaternary glacial sequence in Ecuador: a reinterpretation of the work of Walter Sauer. *Journal of Quaternary Science*, 1:45-56.

DGGM (Dirección General de Geología y Minas), 1978. *Mapas Geológicas de Ecuador, escala 1:100,000*. N. 68-82, Quito, Ecuador.

INECEL, 1988. *Estudio Vulcanológico de "El Reventador"*. Ministerio de Energía y Minas, Quito, Ecuador, 117 pp.

OAQ (Observatorio Astronómico de Quito), 1959. *Breve historia de los principales terremotos de la República del Ecuador*. Publicación del Comité del Año Geofísico Internacional de Ecuador, Quito, Ecuador.

OAQ (Observatorio Astronómico de Quito), 1981. *Catálogo de Sismos del Ecuador, 1900-1980*. Quito, Ecuador.

Pasquarè, G., Tibaldi, A. and Ferrari, L., 1991. Relationships between plate convergence and tectonic evolution of the Ecuadorian active Thrust Belt. In: *Critical Aspects of Plate Tectonic Theory*, edited by S.S. Augusthitis, Theophrastus Publications, Athens, pp. 365-388.

Tibaldi, A., 1990. *Transcurrent tectonics and anomalous volcanic arcs: Analysis of some key areas in Ecuador and Mexico*. Ph.D. Thesis, Università degli Studi di Milano, Italia, (in Italian with an English abstract), 195 pp.

Winter, T. and Lavenu, A., 1989. Morphological and microtectonic evidence for a major active right-lateral strike-slip fault across central Ecuador (South America). *Annales Tectonicae*, III(2):123-139.

Woodward & Clyde Consultant, S. Francisco, Cal., U.S.A., 1981. *Investigaciones para los estudios del riesgo sísmico del sitio de la presa Agoyan*. Technical Report for the Agoyan Dam Project, INECEL, Quito, Ecuador.